

*Department of Industrial Engineering and Management*

## **Technical Report**

No. 2013-10

### ***Perspective reformulation for ship navigation problem***

Kazuhiro Kobayashi and Mirai Tanaka



September, 2013

*Tokyo Institute of Technology*

2-12-1 Ookayama, Meguro-ku, Tokyo 152-8552, JAPAN  
<http://www.me.titech.ac.jp/index-e.html>

# PERSPECTIVE REFORMULATION FOR SHIP NAVIGATION PROBLEM

KAZUHIRO KOBAYASHI AND MIRAI TANAKA

**ABSTRACT.** We present a perspective reformulation of the ship navigation problem, which is a combinatorial network optimization problem to find an efficient shipping route and speed between two ports. The continuous relaxation of our reformulation provides significantly better lower bounds of the objective function. Therefore, better solutions are expected to be obtained faster than the existing formulation. Numerical results are included to illustrate the advantages of our perspective reformulation.

## 1. INTRODUCTION

Recently, the reduction of the fuel consumption has grown in importance since the price of fuel has increased. The fuel consumption depends on a choice of shipping route and shipping speed. Therefore, it is important to optimize them to reduce the fuel consumption in a navigation of a ship. Some researchers have considered problems to optimize shipping speed of a ship in visiting multiple ports. For example, Fagerholt et al. [1] introduced a model to minimize fuel consumption of a ship which visits multiple ports in a voyage. Problems to optimize the shipping speed between two ports also have been investigated. Lo and McCord [2] considered the optimization problem to determine the heading of the ship and its log speed under uncertainty.

In this article, we consider a problem to find an efficient shipping route between two ports and shipping speed on each leg which minimize the total fuel consumption. In practical shipping, the total transition time of a route should be equal to or smaller than the designated time. Therefore, it is necessary to consider not only the total fuel consumption but also the total transition time when determining the shipping route and the speed. We call the problem *ship navigation problem*.

The optimization model for this problem has been considered by Tanaka and Kobayashi [3]. As far as we know, this is the first mixed-integer nonlinear programming model to optimize the shipping route and the speed simultaneously. In their model, the effect of the weather condition to the ship is incorporated in a deterministic way. That is, we assume that the available information correctly depicts the actual weather conditions. If the difference between the information and the actual condition is small, this would provide a reasonable solution. In this article, we employ the same model as in [3].

Let binary variable  $x_{ij}$  becomes unity when the ship moves on arc  $(i, j)$  and zero otherwise, and continuous variable  $v_{ij}$  represents the log speed of the ship on arc  $(i, j)$ . Moreover, let  $r_{ij}$  denote the speed reduction on arc  $(i, j)$ ,  $d_{ij}$  the distance of arc  $(i, j)$ . Then, Tanaka and Kobayashi [3] formulated the problem as the following problem (Orig) on a network:

$$\begin{aligned}
 (1) \quad & \min \sum_{(i,j) \in E} (f_{ij}(v_{ij}) + \tilde{\gamma}_{ij}x_{ij})d_{ij} \\
 (2) \quad & \text{s.t. } v_{\min}x_{ij} \leq v_{ij} \leq v_{\max}x_{ij} \quad ((i, j) \in E), \\
 (3) \quad & x_{ij} \in \{0, 1\} \quad ((i, j) \in E), \\
 (4) \quad & \sum_{(i,j) \in E} \frac{d_{ij}x_{ij}}{v_{ij} - r_{ij}x_{ij}} \leq T, \\
 (5) \quad & \sum_{j:(s,j) \in E} x_{sj} = 1, \\
 (6) \quad & \sum_{j:(i,j) \in E} x_{ij} - \sum_{j:(j,i) \in E} x_{ji} = 0 \quad (i \in V \setminus \{s, t\}), \\
 (7) \quad & \sum_{i:(i,t) \in E} x_{it} = 1,
 \end{aligned}$$

where

$$(8) \quad f_{ij}(v_{ij}) = \tilde{\alpha}_{ij}v_{ij}^2 + \tilde{\beta}_{ij}v_{ij} \quad ((i, j) \in E)$$

and  $E$  denote the set of arcs,  $V$  the set of nodes,  $s$  the source node, and  $t$  the sink node in the network. The objective function (1) minimizes the total fuel consumption. See A. Constraints (2) and (3) ensure that the shipping speed  $v_{ij}$  lies in the disconnected set  $\{0\} \cup [v_{\min}, v_{\max}]$  for given minimum speed  $v_{\min}$  and maximum speed  $v_{\max}$ . Constraint (4) ensures

that the total transition time of an  $s$ - $t$  path is bounded from above with given upper bound  $T$ . Constraints (5), (6) and (7) are the flow conservation constraints.

As we describe later, the problem can be implemented as a mixed-integer second-order cone optimization problem (MISOCP). To solve this problem, we can apply any MISOCP solver. However, it may take long computational time for solving large-scale instances because it usually adopts the branch and bound algorithm. To cope with the difficulty, Tanaka and Kobayashi [3] proposed the route generation algorithm. Their algorithm generates feasible short  $s$ - $t$  paths and then minimizes the fuel consumption by optimizing the shipping speeds on each  $s$ - $t$  path. In this article, we take another approach. We propose a reformulation of the problem which is expected to be solved more efficiently than (1)–(7) by an MISOCP solver.

The remainder of the paper is organized as follows: In Section 2, we give the perspective reformulation of the ship navigation problem and its MISOCP representation. In Section 3, we give the numerical results for evaluating the effectiveness of the proposed perspective reformulation.

## 2. PERSPECTIVE REFORMULATION AND ITS MISOCP REPRESENTATION

When the problem (1)–(7) is solved with a branch and bound algorithm, its continuous relaxation is solved to derive lower bounds on its objective function value. For obtaining better lower bounds, we introduce a tighter formulation of the problem. In the objective function (1) of (Orig),  $f_{ij}(v_{ij})$  is a convex quadratic function. Using a result of [4, 5], we can derive a tighter formulation than (1)–(7) by replacing  $f_{ij}(v_{ij})$  with  $x_{ij}f_{ij}(v_{ij}/x_{ij})$ :

$$\begin{aligned} \min \quad & \sum_{(i,j) \in E} (h_{ij}(v_{ij}) + \tilde{\gamma}_{ij}x_{ij})d_{ij} \\ \text{s.t.} \quad & (2), (3), (4), (5), (6), (7), \\ & h_{ij}(v_{ij}) = x_{ij}f_{ij}\left(\frac{v_{ij}}{x_{ij}}\right). \end{aligned}$$

The function  $h(v_{ij})$  is called the *perspective function* of  $f(v_{ij})$ . Therefore, we call the formulation *perspective reformulation* of (Orig) and denote it by (Persp). The continuous relaxation of (Persp) provides significantly better lower bounds of the objective function than (Orig). Therefore, (Persp) is expected to be solved more efficiently than (Orig) by an MISOCP solver.

Both of the optimization problems (Orig) and (Persp) can be implemented as MISOCPs.

In (Orig), we introduce an auxiliary variable  $w_{ij}$  for each  $(i, j) \in E$  in the objective function. Then, we obtain the following equivalent formulation :

$$\begin{aligned} \min \quad & \sum_{(i,j) \in E} (\tilde{\alpha}_{ij}w_{ij} + \tilde{\beta}_{ij}v_{ij} + \tilde{\gamma}_{ij}x_{ij})d_{ij} \\ \text{s.t.} \quad & (2), (3), (4), (5), (6), (7), \\ (9) \quad & w_{ij} \geq v_{ij}^2 \quad ((i, j) \in E). \end{aligned}$$

Nonlinear constraints in this formulation are (4) and (9). These constraints can be represented as a combination of SOC constraints and a linear constraint. Therefore, (Orig) can be implemented as an MISOCP.

More specifically, in constraint (4), we introduce an auxiliary variable  $s_{ij}$  for each  $(i, j) \in E$ . Then, (4) can be represented as

$$\begin{aligned} (10) \quad & \sum_{(i,j) \in E} d_{ij}s_{ij} \leq T, \\ (11) \quad & \frac{x_{ij}}{v_{ij} - r_{ij}x_{ij}} \leq s_{ij} \quad ((i, j) \in E). \end{aligned}$$

Since  $v_{ij} \geq v_{\min} > r_{ij}$  and  $x_{ij} \in \{0, 1\}$ ,  $v_{ij} - r_{ij}x_{ij} \geq 0$  and  $x_{ij}^2 = x_{ij}$  holds. From these relations, we see that constraint (11) is represented as

$$x_{ij}^2 \leq s_{ij}(v_{ij} - r_{ij}x_{ij}) \quad ((i, j) \in E).$$

Moreover, it can be represented as the second-order cone constraint of the form

$$(12) \quad \begin{pmatrix} s_{ij} + v_{ij} - r_{ij}x_{ij} \\ s_{ij} - v_{ij} + r_{ij}x_{ij} \\ 2x_{ij} \end{pmatrix} \in \mathcal{Q}^3 \quad ((i, j) \in E),$$

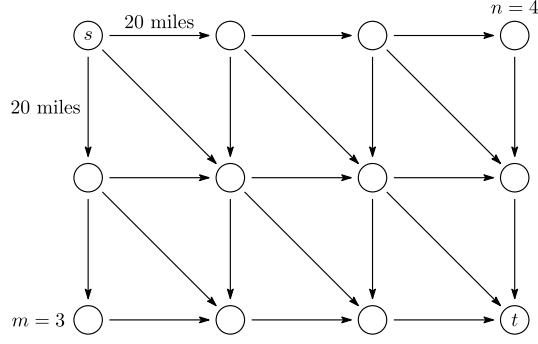


FIGURE 1. Network structure

where  $\mathcal{Q}^3$  is the 3-dimensional second-order cone. In addition, constraint (9) can be represented as the second-order cone constraint of the form

$$(13) \quad \begin{pmatrix} w_{ij} + 1 \\ w_{ij} - 1 \\ 2v_{ij} \end{pmatrix} \in \mathcal{Q}^3 \quad ((i, j) \in E).$$

Consequently, the MISOCP formulation of (Orig) is described as follows:

$$\begin{aligned} \min \quad & \sum_{(i,j) \in E} (\tilde{\alpha}_{ij} w_{ij} + \tilde{\beta}_{ij} v_{ij} + \tilde{\gamma}_{ij} x_{ij}) d_{ij} \\ \text{s.t.} \quad & (2), (3), (5), (6), (7), (10), (12), (13). \end{aligned}$$

Similarly, (Persp) can also be implemented as an MISOCP. In (Persp), we introduce an auxiliary variable  $w_{ij}$  for each  $(i, j) \in A$  in the objective function. Then, we obtain the following equivalent formulation:

$$(14) \quad \begin{aligned} \min \quad & \sum_{(i,j) \in E} (\tilde{\alpha}_{ij} w_{ij} + \tilde{\beta}_{ij} v_{ij} + \tilde{\gamma}_{ij} x_{ij}) d_{ij} \\ \text{s.t.} \quad & (2), (3), (4), (5), (6), (7), \\ & w_{ij} \geq \frac{v_{ij}^2}{x_{ij}} \quad ((i, j) \in E). \end{aligned}$$

Constraint (14) can be represented as the second-order cone constraint of the form

$$(15) \quad \begin{pmatrix} w_{ij} + x_{ij} \\ w_{ij} - x_{ij} \\ 2v_{ij} \end{pmatrix} \in \mathcal{Q}^3 \quad ((i, j) \in E).$$

Consequently, the MISOCP formulation of (Persp) is described as follows:

$$\begin{aligned} \min \quad & \sum_{(i,j) \in E} (\tilde{\alpha}_{ij} w_{ij} + \tilde{\beta}_{ij} v_{ij} + \tilde{\gamma}_{ij} x_{ij}) d_{ij} \\ \text{s.t.} \quad & (2), (3), (5), (6), (7), (10), (12), (15). \end{aligned}$$

### 3. NUMERICAL RESULTS

We performed numerical experiments to show that better solutions of the ship navigation problems can be obtained faster with (Persp) formulation than (Orig) formulation.

The test instances are generated as follows. We consider the grid network illustrated in Figure 1. The network has  $m$  nodes in the vertical direction and  $n$  nodes in the horizontal direction. The value of speed reduction  $r_{ij}$  is a randomly generated integer in  $\{1, 2, 3, 4\}$ . These test instances have been already employed in [3]. In our numerical experiments, we used the same values of  $v_{\min}$ ,  $v_{\max}$ ,  $\alpha$ ,  $\beta$  and  $\gamma$  as those in [1]. Note that the parameters  $\tilde{\alpha}_{ij}$ ,  $\tilde{\beta}_{ij}$ ,  $\tilde{\gamma}_{ij}$  in (Orig) and (Persp) are defined by  $\alpha$ ,  $\beta$ ,  $\gamma$ . See A.

All the numerical tests were performed using Gurobi Optimizer version 5.1 [6] on computer having Intel Xeon 2.80 GHz 6-Core CPUs and 12 GB of RAM with Scientific Linux release 5.9. The time limit of elapsed time in Gurobi Optimizer has been set to 600 seconds.

Table 1 shows the overall numerical results. In the table, we use the following symbols and notations. A pair of figures in “ $m$ ” and “ $n$ ” columns denotes the size of the network. A figure in “ $T$ ” column denotes the value in the right-hand side of total transition time constraint (4). A figure in “time” column denotes the total computational time in seconds. A

TABLE 1. Numerical results

m	n	T	(Persp)			(Orig)			diff
			time	node	gap	time	node	gap	
5	50	90	3.2	0	optimal	600	579927	82.4%	0.2%
5	50	80	19.1	398	optimal	600	82945	137.2%	1.9%
5	50	70	24.0	480	optimal	600	89349	109.9%	1.3%
5	50	60	25.1	679	optimal	600	77288	75.7%	2.0%
5	100	170	40.2	179	optimal	600	42554	170.0%	0.1%
5	100	160	103.8	875	optimal	600	26228	193.0%	0.6%
5	100	150	106.3	821	optimal	600	20670	202.5%	1.8%
5	100	140	103.1	1066	optimal	600	22997	185.1%	1.5%
10	50	90	31.8	521	optimal	600	21894	574.0%	5.8%
10	50	80	76.7	1323	optimal	600	16931	524.1%	11.2%
10	50	70	67.4	861	optimal	600	10942	496.1%	11.2%
10	50	60	58.7	450	optimal	600	3053	383.8%	7.6%
10	100	170	449.4	2240	optimal	600	9236	609.4%	5.5%
10	100	160	404.1	1980	optimal	600	4569	612.0%	7.2%
10	100	150	384.3	1574	optimal	600	5830	589.2%	9.4%
10	100	140	600	2030	2.0%	600	3253	541.6%	12.0%

figure “gap” in column denote the relative difference between the final lower bound  $\underline{\theta}$  and the objective value  $\bar{\theta}$  of the final incumbent defined by  $(\bar{\theta} - \underline{\theta})/\bar{\theta}$ . We use the notation “optimal” to denote that Gurobi optimizer found the optimal solution. A figure in “node” column denote the number of nodes in the search tree. A figure in “diff” column denotes the relative difference in percent between the objective value of the final incumbent of (Orig) formulation  $\bar{\theta}_O$  and that of (Persp) formulation  $\bar{\theta}_P$  defined by  $(\bar{\theta}_O - \bar{\theta}_P)/\bar{\theta}_P$ .

In Table 1, we see that solving with (Persp) formulation provides better solutions faster than (Orig) formulation. More specifically, solving with (Persp) provides optimal solutions for all instances except one with  $m = 5$ ,  $n = 100$ , and  $T = 140$ . In contrast to this, solving with (Orig) does not provide optimal solutions for any instances within 600 seconds.

Figures 2 and 3 show the results for (Orig) formulation and (Persp) formulation on the instance with  $m = 5$ ,  $n = 100$ , and  $T = 140$ , respectively. In these figures, we plotted the computational times on the horizontal axes and the objective values of the incumbents (denoted by “Incumbent”) and the lower bounds (denoted by “BestBd”) on the vertical axes. From Figure 2, we see that (Orig) formulation did not provide good lower bounds. In contrast to this, from Figure 3, we see that (Persp) formulation provided good lower bounds in early iterations. Moreover, an optimal solution has been obtained.

In Figures 4 and 5, we plotted the numbers of nodes in the search trees for solving the same instance with (Orig) formulation and with (Persp) formulation, respectively. In these figures, the horizontal axes give the computational times and the the vertical axes give the numbers of unexplored nodes (denoted by “Unexpl”) and the numbers of explored nodes (denoted by “Expl”).

From Figure 4, we see that both of the number of unexplored nodes and that of explored nodes for (Orig) formulation grow large, which is nearly proportional to the computational time. In contrast to this, from Figure 5, we see that the number of unexplored nodes remains small for (Persp) formulation. This indicates the effectiveness of the the bounding process in solving (Persp) formulation.

#### APPENDIX A. COEFFICIENTS OF THE OBJECTIVE FUNCTION

Here, we show the relationship between  $\tilde{\alpha}$ ,  $\tilde{\beta}$ , and  $\tilde{\gamma}$  in (Orig) and (Persp) and  $\alpha$ ,  $\beta$ , and  $\gamma$  in [1]. In [1], the fuel consumption per unit time on arc  $(i, j)$  is expressed by the cubic function  $\alpha v_{ij}^3 + \beta v_{ij}^2 + \gamma v_{ij}$  of log speed  $v_{ij}$ . When the speed reduction on arc  $(i, j)$  is  $r_{ij}$ , the ground speed is  $v_{ij} - r_{ij}$ . Then, the fuel consumption on arc  $(i, j)$  is given by

$$\frac{\alpha v_{ij}^3 + \beta v_{ij}^2 + \gamma v_{ij}}{v_{ij} - r_{ij}} d_{ij}.$$

The function is approximated by a convex quadratic function [3]

$$(\tilde{\alpha}_{ij} v_{ij}^2 + \tilde{\beta}_{ij} v_{ij} + \tilde{\gamma}_{ij} x_{ij}) d_{ij}$$

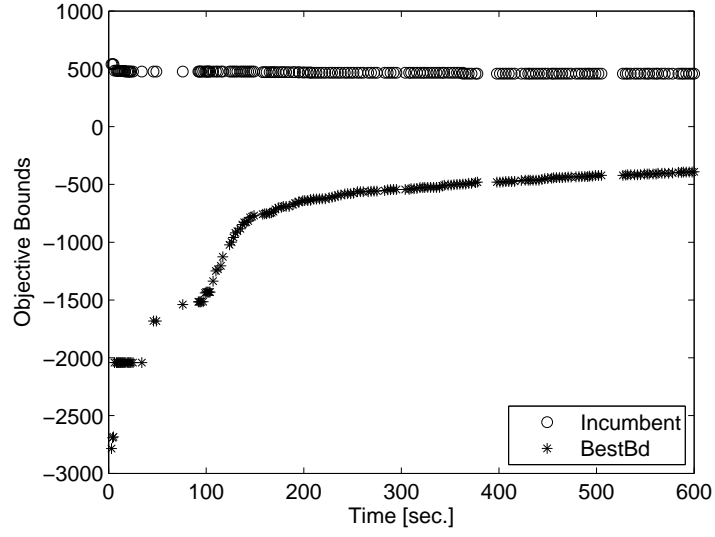


FIGURE 2. Incumbents and lower bounds for (Orig)

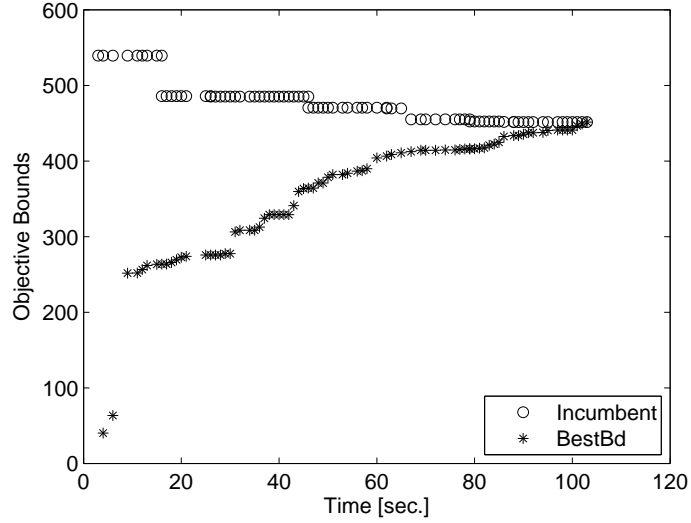


FIGURE 3. Incumbents and lower bounds for (Persp)

by using Taylor approximation at  $v = \bar{v} = (v_{\min} + v_{\max})/2$ . The coefficients  $\tilde{\alpha}_{ij}$ ,  $\tilde{\beta}_{ij}$  and  $\tilde{\gamma}_{ij}$  are given by

$$\begin{aligned}\tilde{\alpha}_{ij} &= \alpha + \frac{\delta_{ij}}{(\bar{v} - r_{ij})^3}, \\ \tilde{\beta}_{ij} &= \beta'_{ij} - \frac{\delta_{ij}}{(\bar{v} - r_{ij})^2} - 2\frac{\delta_{ij}}{(\bar{v} - r_{ij})^3}\bar{v}, \\ \tilde{\gamma}_{ij} &= \gamma'_{ij} + \frac{\delta_{ij}}{\bar{v} - r_{ij}} + \frac{\delta_{ij}}{(\bar{v} - r_{ij})^2}\bar{v} + \frac{\delta_{ij}}{(\bar{v} - r_{ij})^3}\bar{v}^2,\end{aligned}$$

where

$$\begin{aligned}\beta'_{ij} &= \alpha r_{ij} + \beta, \\ \gamma'_{ij} &= \alpha r_{ij}^2 + \beta r_{ij} + \gamma, \\ \delta_{ij} &= \alpha r_{ij}^3 + \beta r_{ij}^2 + \gamma r_{ij}.\end{aligned}$$

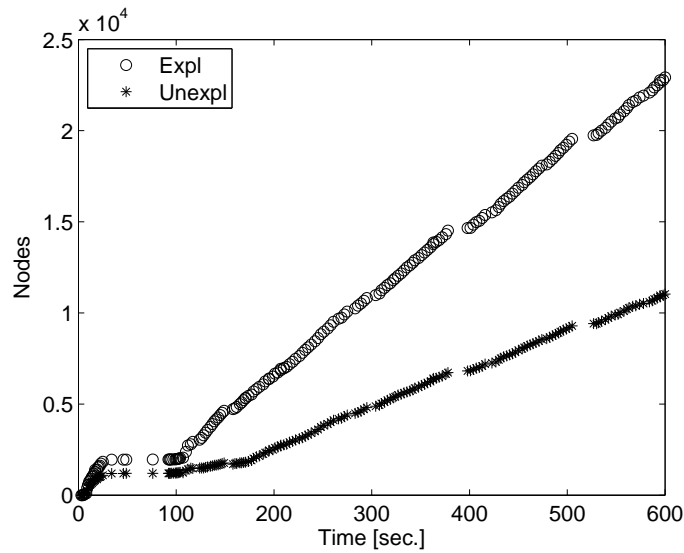


FIGURE 4. Number of nodes in the search tree for (Orig)

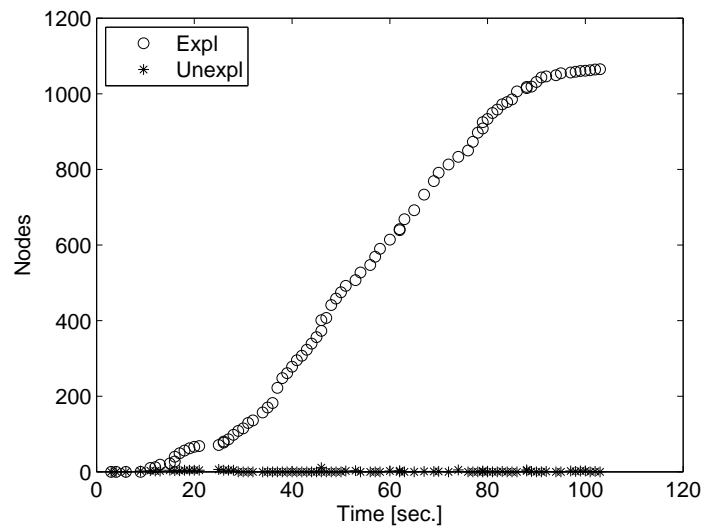


FIGURE 5. Number of nodes in the search tree for (Persp)

#### REFERENCES

- [1] K. Fagerholt, G. Laporte, I. Norstad, Reducing fuel emissions by optimizing speed on shipping routes, *J. Oper. Res. Soc.* 61 (2010) 523–529.
- [2] H. Lo, M. McCord, Adaptive ship routing through stochastic ocean current: general formulations and empirical results, *Transp. Res. A* 32 (7) (2003) 138–156.
- [3] M. Tanaka, K. Kobayashi, MISOCP formulation and route generation algorithm for ship navigation problem, Tech. Rep. 2013-8, Dep. of Industrial Engineering and Management, Tokyo Institute of Technology (2013).
- [4] A. Frangioni, C. Gentile, Perspective cuts for a class of convex 0-1 mixed integer programs, *Math. Program.* 106 (2006) 225–236.
- [5] O. Günlük, J. Linderoth, Perspective reformulations of mixed integer nonlinear programs with indicator variables, *Math. Program.* 124 (1-2) (2010) 183–205.
- [6] Gurobi, Gurobi optimizer reference manual, <http://www.gurobi.com> (2013).

(Kobayashi, K.) NAGIVATION & LOGISTICS ENGINEERING DEPARTMENT, NATIONAL MARITIME RESEARCH INSTITUTE, 6-38-1 SHINKAWA, MITAKA-SHI, TOKYO, 181-0004, JAPAN  
*E-mail address:* kobayashi@nmri.go.jp

(Tanaka, M.) GRADUATE SCHOOL OF DECISION SCIENCE AND TECHNOLOGY, TOKYO INSTITUTE OF TECHNOLOGY, 2-12-1-W9-60, OOKAYAMA, MEGURO-KU, TOKYO, 152-8552, JAPAN  
*E-mail address:* tanaka.m.aa@m.titech.ac.jp